Phase Transitions in the Distribution of Bipartite Entanglement of a Random Pure State

Celine Nadal[1], Satya N. Majumdar[1] and Massimo Vergassola[2]
[1] *Laboratoire de Physique Théorique et Modèles Statistiques (UMR 8626 du CNRS), Université Paris-Sud, Bâtiment 100, 91405 Orsay Cedex, France.*
[2] *Institut Pasteur, CNRS URA 2171, F-75724 Paris 15, France.*
(Dated: November 17, 2009)

Using a Coulomb gas method, we compute analytically the probability distribution of the Renyi entropies (a standard measure of entanglement) for a random pure state of a large bipartite quantum system. We show that, for any order $q > 1$ of the Renyi entropy, there are two critical values at which the entropy's probability distribution changes shape. These critical points correspond to two different transitions in the corresponding charge density of the Coulomb gas : the disappearance of an integrable singularity at the origin and the detachement of a single-charge drop from the continuum sea of all the other charges. These transitions respectively control the left and right tails of the entropy's probability distribution, as verified also by Monte Carlo numerical simulations of the Coulomb gas equilibrium dynamics.

PACS numbers: 02.50.-r, 02.50.Sk, 03.67.Mn, 02.10.Yn

Entanglement is a crucial resource in quantum information and computation [1] as a measure of nonclassical correlations between different parts of a quantum system. To exploit such correlations to the maximum advantage in quantum algorithms, it is desirable to create states with large entanglement. A potential candidate for such a state is a bipartite *random* pure state, its *average* entanglement entropy being almost maximal [2, 3]. Such a random pure state can also be used as a null model or reference point to which the entanglement of an arbitrary time-evolving quantum state may be compared. In addition, such random states are also relevant in quantum chaotic or non-integrable systems [4, 5].

The conclusion that a random pure state in a bipartite system has near maximal entropy is based only on the result for the *average* entropy [2, 3]. Even though the average entropy of the random state may be *close* to its maximal value, the probability of the *closeness* may actually be very small (see below). The quantitative evaluation of this probability requires to compute the full probability distribution of the entropy, namely its large deviation tails. In addition, the distribution of bipartite entanglement may also be used to characterize entanglement in a multipartite system [6, 7]. In this Letter we compute the full distribution of the Renyi entanglement entropies (defined later) for random pure states of a bipartite system. The calculation is realized using a Coulomb gas method and is valid in the limit when both subsystems are large. A by-product of our results is the behavior of the probability that the entropy approaches its maximal value $\ln N$.

We start with a standard bipartite system $A \otimes B$ composed of two smaller subsystems A and B, whose respective Hilbert spaces $\mathcal{H}_A^{(N)}$ and $\mathcal{H}_B^{(M)}$ have dimensions N and M. For simplicity, we focus on the $N = M$ case, though all our results can be extended to the $N \neq M$ case. Let $|\psi\rangle$ be a normalized pure state of the full system with its density matrix $\rho = |\psi\rangle\langle\psi|$ satisfying $\mathrm{Tr}[\rho] = 1$. The two reduced density matrices are denoted $\rho_A = \mathrm{Tr}_B[\rho]$ and $\rho_B = \mathrm{Tr}_A[\rho]$. It is not difficult to prove that both ρ_A and ρ_B share the same set of non-negative eigenvalues $\{\lambda_1, \lambda_2, \ldots, \lambda_N\}$ with $\sum_{i=1}^N \lambda_i = 1$. Let $|\lambda_i^A\rangle$ and $|\lambda_i^B\rangle$ denote the respective eigenvectors of ρ_A and ρ_B. In this so-called Schmidt basis, an arbitrary pure state can be represented as

$$|\psi\rangle = \sum_{i=1}^{N} \sqrt{\lambda_i}\, |\lambda_i^A\rangle \otimes |\lambda_i^B\rangle. \tag{1}$$

This representation is very useful for characterizing the entanglement between A and B. For example, consider two opposite limiting situations: (i) One of the eigenvalues, say λ_i, is unity and the remaining $N-1$ are identically zero. Then, $|\psi\rangle = \sqrt{\lambda_i}\,|\lambda_i^A\rangle \otimes |\lambda_i^B\rangle$ factorizes and the system is completely *unentangled*. (ii) All eigenvalues are equal ($\lambda_i = 1/N$ for all i). Then, all the states are equally present in Eq. (1) and the state $|\psi\rangle$ is *maximally* entangled. A standard measure of entanglement is the von Neumann entropy, $S_{VN} = -\sum_i \lambda_i \ln \lambda_i$, which takes its minimum value 0 in situation (i) and its maximal value $\ln N$ in situation (ii). Another useful measure of entanglement is provided by Renyi's entropies, the quantities of major interest here :

$$S_q = \frac{1}{1-q} \ln \left[\sum_{i=1}^{N} \lambda_i^q \right], \tag{2}$$

which also attain their minimum value 0 in situation (i) and their maximum value $\ln N$ in (ii). As $q \to 1$ and $q \to \infty$, the Renyi entropy tends respectively to the von Neumann entropy S_{VN} and $-\ln \lambda_{\max}$, where $\lambda_{\max}$ is the largest eigenvalue.

A pure state $|\psi\rangle$ is called *random* when it is sampled according to the uniform Haar measure (the unique unitarily invariant measure) over the full Hilbert space. As a result, the eigenvalues $\{\lambda_i\}$'s also become random variables with the joint distribution (for $M = N$) [3] :

$$P[\{\lambda_i\}] = \frac{1}{Z_0} \prod_{i=1}^{N} \lambda_i^{\frac{\beta}{2}-1} \prod_{j<k} |\lambda_j - \lambda_k|^\beta \delta\left(\sum_{i=1}^{N} \lambda_i - 1 \right). \tag{3}$$

Here, $\beta = 2$ and the δ-function enforces the unit trace constraint $\mathrm{Tr}[\rho_A] = 1$. Apart from this constraint, (3) is identical to the eigenvalue distribution of random Gaussian Wishart

(covariance) matrices. For random matrices, the Dyson index β takes the values 1, 2 or 4 depending on whether the matrix is real, complex or quaternion. Hence, we shall study (3) for general β, even though $\beta = 2$ in the quantum context. The normalization constant Z_0 can be computed exactly using Selberg's integrals [8] as $Z_0 \sim e^{-\beta N^2/4}$, to leading order in N.

Since the λ_i's are random variables distributed as in (3), the von Neumann and the Renyi entropies in (2) are also random variables. Statistical properties of these observables, as well as others such as concurrence, purity, minimum eigenvalue etc., have been studied extensively [2, 3, 6, 7, 8, 9, 10, 11]. In particular, the average von Neumann entropy $\langle S_{VN} \rangle = \ln N - 1/2$, is close for large N to its maximum value [3]. In contrast, few studies have addressed the full distribution of the entropy, an exception being the purity $\Sigma_2 = \sum_{i=1}^{N} \lambda_i^2$: for small N, the distribution of purity is known exactly [9]; for large N, the Laplace transform of the purity distribution was studied recently for positive Laplace variables [7]. However, the inverse Laplace transform of this quantity provides only partial information about the purity distribution.

The goal of our Letter is to compute analytically, for large N and all $q > 1$, the full distribution of the Renyi entropies in (2), or equivalently of $\Sigma_q = \sum_{i=1}^{N} \lambda_i^q = \exp[(1-q)S_q]$. The quantities Σ_q satisfy the inequalities $N^{1-q} \leq \Sigma_q \leq 1$ for $q > 1$, with the upper and lower bounds corresponding to the unentangled (i) and the maximally entangled (ii) situations. The distribution of Σ_q is written using (3) as

$$P(\Sigma_q, N) = \int P[\{\lambda_i\}] \delta \left(\sum_i \lambda_i^q - \Sigma_q \right) \prod_i d\lambda_i \,. \qquad (4)$$

The approach we employed to treat (4) is a saddle-point method to identify the configuration of the eigenvalues $\{\lambda_i\}$'s that dominates for large N. Configurations at large N are characterized by the continuous density $\rho(\lambda, N) = N^{-1} \sum_i \delta(\lambda - \lambda_i)$ and the main challenge, accomplished here, is to find the saddle-point density $\rho_c(\lambda, N)$.

Let us first summarize our main results. The normalization $\sum_{i=1}^{N} \lambda_i = 1$ implies that the typical amplitude of the eigenvalues $\lambda_i \sim 1/N$ and hence $\Sigma_q \sim N^{1-q}$ for large N. We define then the rescaled intensive variable $s \equiv N^{q-1} \Sigma_q$ whose lowest value $s = 1$ corresponds to the maximally entangled situation (ii). In Fig. 1, a typical plot of $P(\Sigma_q = N^{1-q} s, N)$ vs s is shown for large N and fixed $q > 1$: the distribution has a Gaussian peak flanked on both sides by non-Gaussian tails. Specifically, we find two critical values $s = s_1(q)$ and $s = \bar{s}(q)$ separating three regimes I ($1 \leq s \leq s_1(q)$), II ($s_1(q) \leq s \leq \bar{s}(q)$) and III ($s > \bar{s}(q)$). At the first critical point $s_1(q)$ the distribution has a weak singularity (third derivative is discontinuous). At the second critical point $\bar{s}(q)$, a Bose-Einstein type condensation transition occurs (see below). These changes are a direct consequence of two phase transitions in the associated optimal charge density (shown in Fig. 2). In regime I, the optimal charge density has a compact support $[\zeta_1/N, \zeta_2/N]$, where ζ_1 is strictly positive (Fig. 2a).

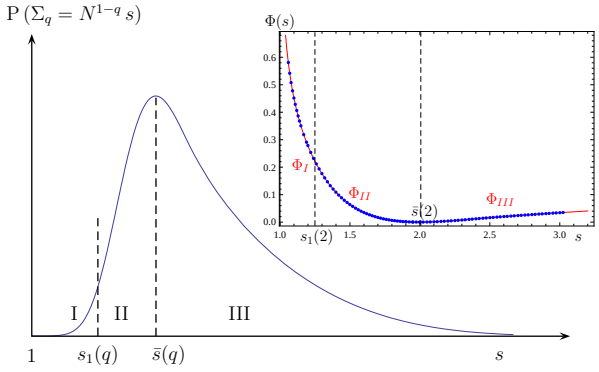

FIG. 1: The schematic distribution of $\Sigma_q = N^{1-q} s = \sum_{i=1}^{N} \lambda_i^q$ as a function of s for fixed large N. Two critical points $s = s_1(q)$ and $s = \bar{s}(q)$ separate three regimes I, II and III characterized by the different optimal densities shown in Fig. 2. The maximally entangled state $s = 1$ is at the extreme left, in the large deviation tail well-spaced from the average $\bar{s}(q)$. (Inset) The large deviation functions Φ for the distribution of Σ_q, in the three different regimes. Analytical predictions (red solid line) are compared to the results (blue points) of Monte Carlo numerical simulations of the Coulomb gas equilibrium dynamics.

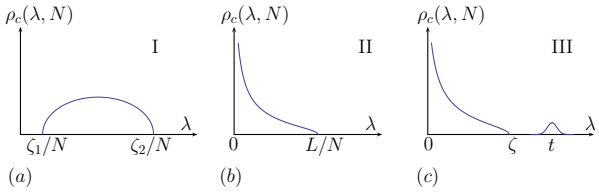

FIG. 2: Scheme of the optimal saddle-point density ρ_c of the eigenvalues, or equivalently of the Coulomb gas charges, for $1 \leq s \leq s_1(q)$ (regime I), $s_1(q) \leq s \leq \bar{s}(q)$ (II) and $s > \bar{s}(q)$ (III). In the regime III, the maximum eigenvalue becomes larger than all the others ($\sim O(1/N)$), as shown by the isolated bump at t in (2c).

When the control parameter s exceeds $s_1(q)$ (regime II), the left edge of the support sticks to zero while the upper edge L/N moves to the right as s increases (Fig. 2b), till the second critical value $\bar{s}(q)$ corresponding to $L = 4$. For $s > \bar{s}(q)$ (regime III), we find that one eigenvalue (the small bump in Fig. 2c) splits off the sea of all the other $N-1$ eigenvalues, which remain $\sim O(1/N)$. This second phase transition is reminiscent of the real-space condensation phenomenon observed in a class of lattice models for mass transport, where a single lattice site carries a thermodynamically large mass [12].

Note that for $q = 2$, the presence of two phase transitions was also noticed in Ref. [7] for the Laplace transform of the distribution $P(\Sigma_2, N)$. However, the nature of the regime III was not elucidated and the corresponding optimal density and the partition function were not calculated. To derive the full distribution $P(\Sigma_2, N)$, one needs the partition function in all three regimes, which is what we do here for all $q > 1$ at large N. We also find exact expressions for the two critical points: $4^{-q} \bar{s}(q) = \Gamma(q + 1/2)/(\sqrt{\pi}\Gamma(q+2))$ and $(4(q+1)/3q)^{-q} s_1(q) = \Gamma(q + 3/2)/(\sqrt{\pi}\Gamma(q+2))$. From

the Gaussian form near the peak $s = \bar{s}(q)$, we also read off the mean and the variance of the entropy S_q for all q:

$$\langle S_q \rangle \approx \ln(N) - \frac{\ln \bar{s}(q)}{q-1}; \quad \mathrm{Var}(S_q) \approx \frac{q}{2\beta N^2}. \qquad (5)$$

Let us now briefly outline how the previous results are derived. By using (3) and (4), we obtain

$$P(\Sigma_q, N) = \frac{Z(\Sigma_q)}{Z_0}\,;\; Z(\Sigma_q) = \int e^{-\beta E(\{\lambda_i\})} \prod_i d\lambda_i\,, \quad (6)$$

with $E(\{\lambda_i\}) = -(1/2-1/\beta)\sum_i \ln(\lambda_i) - \sum_{i<j} \ln|\lambda_i - \lambda_j|$ and the integral runs over the subspace satisfying the two constraints, $\sum_i \lambda_i = 1$ and $\sum_i \lambda_i^q = \Sigma_q$. The expression for $E(\{\lambda_i\})$ is interpreted as the energy of a Coulomb gas of charged particles with coordinates λ_i that repel each other via 2-d logarithmic interactions and are also subject to an external logarithmic potential. In the large N limit, we can characterize the configuration of the Coulomb gas' charges by the normalized density $\rho(\lambda, N) = N^{-1}\sum_i \delta(\lambda - \lambda_i)$. Due to the constraint $\sum_i \lambda_i = 1$, typically $\lambda_i \sim 1/N$. Hence, the charge density scales as $\rho(\lambda, N) \approx N\,\rho(\lambda N)$ and we introduce the rescaled variable $s \equiv N^{q-1}\Sigma_q$. We then replace the multiple integral in (4) by a functional integral over all possible normalized and rescaled charge density functions $\rho(x)$ satisfying the three constraints: $\int \rho(x)dx = 1$, $\int x\rho(x)dx = 1$ and $\int x^q \rho(x)dx = s$. The resulting functional integral over $\rho(x)$ is evaluated in the large N limit via the saddle point method. This constrained Coulomb gas approach has been used successfully in a variety of contexts that include the distribution of the top eigenvalues of Gaussian and Wishart matrices [13, 14, 15], phase transition in the restricted trace ensemble [16], purity partition function in bipartite systems [7], nonintersecting Brownian interfaces [17], quantum transport in chaotic cavities [18], information and communication systems [19], and the index distribution for Gaussian random fields [20, 21] and Gaussian matrices [22].

The constrained Coulomb gas approach yields $P\left(\Sigma_q = N^{1-q}\,s\right) \propto \int \mathcal{D}[\rho]\; e^{-\beta N^2 E_s[\rho]}$. To the leading order in N, the effective energy reads

$$E_s[\rho] = -\frac{1}{2}\int_0^\infty\!\!\int_0^\infty dx\,dx'\rho(x)\rho(x')\ln|x-x'| + \mu_0\left(\int_0^\infty dx\rho(x) - 1\right) + \mu_1\left(\int_0^\infty dx x\rho(x) - 1\right) + \mu_2\left(\int_0^\infty dx x^q\rho(x) - s\right), \quad (7)$$

where the Lagrange multipliers μ_0, μ_1 and μ_2 enforce the constraints. For large N, the method of steepest descent gives: $P\left(\Sigma_q = N^{1-q}\,s\right) \propto e^{-\beta N^2 E_s[\rho_c]}$ where $\rho_c(x)$ minimizes the energy: $\delta E_s[\rho]/\delta\rho = 0$. This gives the integral equation

$$V(x) = \mu_0 + \mu_1 x + \mu_2 x^q = \int_0^\infty \rho_c(x')\ln|x-x'|dx'\,, \quad (8)$$

with $V(x)$ acting like an effective external potential. Differentiating once more with respect to x leads to

$$\mu_1 + q\mu_2 x^{q-1} = \mathcal{P}\int_0^\infty \frac{\rho_c(x')}{x-x'}dx'\,, \qquad (9)$$

where $\mathcal{P}$ denotes Cauchy's principal part. The single-support solution to (9) is found by using Tricomi formula [23] and yields the regimes sketched in Figs. 1 and 2.

Regime I: For $1 \le s \le s_1(q)$, we find that $\mu_1 < 0$, $\mu_2 > 0$ and the effective potential $V(x)$ has a minimum at a nonzero x. This indicates that the charges concentrate around this nonzero minimum over a support $[\zeta_1, \zeta_2]$ for all $q > 1$ (see Fig. 2a). For $q = 2$, the edges $\zeta_{1,2} = 1 \mp 2\sqrt{s-1}$ and the solution $\rho_c(x) = \sqrt{(\zeta_2 - x)(x - \zeta_1)}/(2\pi(s-1))$ vanishes at both edges. This solution exists for $\zeta_1 > 0$, i.e., for $s < s_1(2) = 5/4$, and the distribution $P(\Sigma_2 = s/N, N) \sim e^{-\beta N^2 \Phi_I(s)}$ with the large deviation function

$$\Phi_I(s) = -\frac{1}{4}\ln(s-1) - \frac{1}{8}. \qquad (10)$$

The behavior for $q \neq 2$ is qualitatively similar, though the expressions are cumbersome [24]. Setting $s = 1 + \epsilon$ around the maximal entropy state $s = 1$, the probability at this extreme left tail scales as $\sim \epsilon^{\beta N^2/4}$, i.e. it is very small for large N. As s approaches $s_1(q)$ from below, μ_1 and the minimum of $V(x)$ tend to zero. This signals that the charges now concentrate near the origin and the onset of regime II.

Regime II: For $s_1(q) \le s \le \bar{s}(q)$, the charges concentrate over a support $[0, L]$ (see Fig. 2b). For $q = 2$, the optimal charge density takes the simple form $\rho_c(x) = \sqrt{(L-x)}(A + Bx)/(\pi\sqrt{x})$, where $A = 4(L-2)/L^2$, $B = 8(4-L)/L^3$ and the right edge $L = 6 - 2\sqrt{9-4s}$. Evaluating the energy for large N, we get $P(\Sigma_2 = s/N, N) \sim e^{-\beta N^2 \Phi_{II}(s)}$ with

$$\Phi_{II}(s) = -\frac{1}{2}\ln(L/4) + \frac{6}{L^2} - \frac{5}{L} + \frac{7}{8}\,. \qquad (11)$$

Comparing (10) and (11), it is verified that the large deviation functions match at the critical point $s_1 = 5/4$ up to the second derivative, while the third is discontinuous: $\Phi_I^{(3)}(5/4) = -32$ and $\Phi_{II}^{(3)}(5/4) = -16$. The function $\Phi_{II}(s)$ is quadratic $\Phi_{II}(s) \approx (s-2)^2/8$ around its minimum at $s = \bar{s}(2) = 2$. Thus, the distribution $P(\Sigma_2 = s/N, N)$ has a Gaussian peak near $s = 2$, with the mean $\langle \Sigma_2 \rangle = 2/N$ and the variance $\mathrm{Var}(\Sigma_2) = 4/(\beta N^4)$ for large N. The corresponding expressions for arbitrary $q > 1$ are given in (5).

For any $q > 1$, μ_1 is positive, $\mu_2 \to 0$ as $s \to \bar{s}(q)$ and $\mu_2 < 0$ for $s > \bar{s}(q)$. This indicates that the potential $V(x)$ in

(8) becomes non-monotonic for $s > \bar{s}(q)$: it increases around the origin, reaches a maximum at $x^* = (-\mu_1/q\mu_2)^{1/(q-1)}$ and then decreases monotonically for $x > x^*$. It follows that the minimum at $x = 0$ as well as the associated saddle-point solution become *metastable*. This solution still exists over a finite range for $s > \bar{s}(q)$ (e.g., for $q = 2$ over $2 \leq s \leq 9/4$). For $s > \bar{s}(q)$, however, there is a second *stable* solution where one eigenvalue splits off the sea of the remaining $(N-1)$ eigenvalues (see regime III below). For $s > \bar{s}(q)$, the energy associated with this stable solution is lower by $\sim O(1/N)$ only, as compared to the energy of the metastable solution.

Regime III: For $s > \bar{s}(q)$, the correct density of states consists of two disjoint parts: (a) $(N-1)$ eigenvalues remain $\sim O(1/N)$, concentrated over a finite support including the origin; (b) the top eigenvalue $\lambda_{\max}$ takes a larger value and moves away from the sea of all the others (see Fig. 2c). The saddle point method thus needs to be slightly revised. For simplicity, let us focus only on $q = 2$. We write $\lambda_{\max} = t$ and label the remaining $(N-1)$ eigenvalues by their continuous density $\rho(\lambda) = \frac{1}{N-1} \sum_{i \neq max} \delta(\lambda - \lambda_i)$. We then express the energy $E[\{\lambda_i\}]$ in (6) in terms of $\rho(\lambda)$ and t, treating both of them as variables. This gives $P(\Sigma_2 = S, N) \propto \int \mathcal{D}\rho \int dt \; e^{-\beta H_S[\rho,t]}$, where the effective energy $H_S[\rho, t]$ has a long expression that includes ρ, t and three Lagrange multipliers enforcing the constraints [24]. Assuming that $\rho(\lambda)$ has a finite support over $[0, \zeta]$ with $\zeta < t$, we minimize the effective energy over both ρ and t. The equations $\delta H_S/\delta\rho = 0 = \partial H_S/\partial t$ are solved again using Tricomi's theorem [23]. Substituting the solutions for $\rho(\lambda)$ and t in the effective energy finally yields the distribution $P(\Sigma_2, N)$ at the leading order in N. We have verified that in the regime $2 \leq s \leq 9/4$, the resulting distribution coincides with that of regime II, i.e. the transition at $\Sigma_2 \to 2/N$ is smooth. The maximum eigenvalue $\lambda_{\max} = t$ dominates at the upper edge of the regime III, when $\Sigma_2 \sim O(1)$, and we find [24] that $P(\Sigma_2 = S, N) \sim (1 - \sqrt{S})^{\beta N^2/2}$.

Numerical Simulations. To verify analytical predictions, we simulated the distribution (3) of the eigenvalues λ_i, which is interpreted as the Boltzmann weight of a Coulomb gas and sampled using the Metropolis algorithm (see, e.g., [25]). Specifically, we start with a configuration of the λ_i's satisfying $\sum_i \lambda_i = 1$. The moves in the Metropolis scheme consist of picking at random a pair (λ_i, λ_j) and proposing to modify them as $(\lambda_i + \varepsilon, \lambda_j - \varepsilon)$ where ε is set to achieve the standard average rejection rate $1/2$ [25]. As usual, the move is accepted with probability $e^{-\beta \Delta E}$ if $\Delta E > 0$ and with probability 1 if $\Delta E < 0$, where ΔE is the change in energy $E[\{\lambda_i\}]$ (the move is rejected if one of the eigenvalues becomes negative). This ensures that at long times we reach thermal equilibrium with the correct Boltzmann weight $\propto e^{-\beta E[\{\lambda_i\}]}$ satisfying the constraint $\sum_i \lambda_i = 1$. We then construct the histogram of $P(\Sigma_q = \sum_i \lambda_i^q, N)$. Numerical data compare very well with our analytical predictions (see the inset of Fig. 1 for $q = 2$, $N = 50$); we also verified that a single eigenvalue detaches from the sea in regime III (intuitively, multiple drops are unfavorable as they compress the sea more than a single drop due to the convexity of $\sum \lambda_i^q$ for $q > 1$).

In conclusion, we have obtained the first complete characterization of the quantum entanglement's statistical properties in a bipartite random pure state of large dimensions N. The average of the Renyi entropies is indeed close to its largest value $\ln N$. This is, however, the mere consequence of the typical amplitude $1/N$ of the density matrix eigenvalues. The distribution of the eigenvalues mostly affects the $O(1)$ contribution to the entropy. The probability to approach $\ln N$ is actually found to decay rapidly at large N, as clearly shown by the full probability distribution of the Renyi entropies derived here. The spreading of the eigenvalues becomes prominent in the regime III (in Figs. 1 and 2) where a condensation occurs and the contribution by the single top eigenvalue of the density matrix is thermodynamically relevant.

Acknowledgements We thank O. Bohigas and A. Scardicchio for useful discussions.

[1] M.A. Nielsen and I.L. Chuang, *Quantum Computation and Quantum Information* (Cambridge Univ. Press, Cambridge, 2000).

[2] E. Lubkin, J. Math. Phys. **19**, 1028 (1978); S. Lloyd and H. Pagels, Ann. Phys. (N.Y.) **188**, 186 (1988).

[3] D.N. Page, Phys. Rev. Lett. **71**, 1291 (1993).

[4] O. Bohigas, M. J. Giannoni and C. Schmit, Phys. Rev. Lett. **52**, 1 (1984).

[5] J.N. Bandyopadhyay and A. Lakshminarayan, Phys. Rev. Lett. **89**, 060402 (2002) and references therein.

[6] P. Facchi, G. Florio, G. Parisi and S. Pascazio, Phys. Rev. A **77**, 060304 (R) (2008).

[7] P. Facchi et al., Phys. Rev. Lett. **101**, 050502 (2008).

[8] K. Zyczkowski and H-J. Sommers, J. Phys. A: Math. Gen. **34**, 7111 (2001).

[9] O. Giraud, J. Phys. A.: Math. Theor. **40**, 1053 (2007).

[10] M. Znidaric, J. Phys. A: Math. Theor. **40**, F105 (2007).

[11] S.N. Majumdar, O. Bohigas, and A. Lakshminarayan, J. Stat. Phys. **131**, 33 (2008).

[12] S.N. Majumdar, M.R. Evans and R.K.P. Zia, Phys. Rev. Lett. **94**, 180601 (2005).

[13] D.S. Dean and S.N. Majumdar, Phys. Rev. Lett. **97**, 160201 (2006); Phys. Rev. E **77**, 41108 (2008).

[14] P. Vivo, S.N. Majumdar and O. Bohigas, J. Phys. A: Math. Theor. **40**, 4317 (2007).

[15] S.N. Majumdar and M. Vergassola, Phys. Rev. Lett. **102**, 060601 (2009).

[16] G. Akemann et al., Phys. Rev. E **59**, 1489 (1999).

[17] C. Nadal and S.N. Majumdar, Phys. Rev. E **79**, 061117 (2009).

[18] P. Vivo, S.N. Majumdar and O. Bohigas, Phys. Rev. Lett. **101**, 216809 (2008); arXiv:0909:2974 (2009).

[19] P. Kazakopoulos et al., [arXiv:0907.5024] (2009).

[20] A.J. Bray and D.S. Dean, Phys. Rev. Lett. **98**, 150201 (2007).

[21] Y.V. Fyodorov and I. Williams, J. Stat. Phys. **129**, 1081 (2007).

[22] S.N. Majumdar et al., [arXiv:0910:0775] (2009).

[23] F.G. Tricomi, *Integral Equations* (Pure Appl. Math. V, Interscience, London, 1957).

[24] Details will be published elsewhere.

[25] W. Krauth, *Statistical Mechanics: Algorithms and Computation* (Oxford Univ. Press, Oxford, 2006).